Scanned-Forward-Looking Method for Automatic Centerline Extraction in Virtual Endoscopy

Gabriel PREDA, Radu Cristian POPA, Catalin CIOBOTARU
Advantec Solutions, Titulescu 89-91, Bucharest, Romania

Radu MARIAN, M.D.
Clinical Emergency Hospital - Bucharest, Floreasca 8, Bucharest, Romania

Alexandru POPIEL, M.D.
Emergency Hospital "Bagdasar-Arseni", Berceni 12, Bucharest, Romania

Abstract. Organ exploration in virtual endoscopy ideally involves calculating an optimally central path through the anatomical cavity under investigation. The path represents the guiding support for the virtual camera that inspects the inner details of the organ. We introduce in this paper a robust and efficient method for automatic generation of a quality centerline in organs of complex geometries. The algorithm neuromimetically combines the usually employed lateral information with a "scanned-forward-looking" information to construct point-by-point a continuous and branch-free navigation trajectory that is optimal on both criteria. Almost all the computational effort is spent on computing the distance map of the object.

1 Introduction

The success of modern virtual endoscopy relies on the progress in several processing steps, such as 3D data packing and resampling, smoothing and noise filtering, organ segmentation, fast and flexible rendering, and stable, deterministic inner navigation. The construction of an optimal centerline in a complex anatomical structure is a still open problem. Not only the quality of the path evaluation is essential, but also the stability (robustness) to shape variations and the computational effort involved.

The exploration trajectory must comply with easily defined criteria: uniformly staying away from the boundary, continuity, single-voxel (or zero) thickness, no looping and branching, smoothness. In case of non-ideal geometries - as is the case with most of the anatomical cavities - finding a smooth "central" path becomes a problem with multiple solutions.

Most of the existing centerline extraction methods can be classified into three categories: manual extraction, topological thinning, and processing based on distance maps. Manual extraction requires the user to identify and pick the succession of points that define the path. Even though it is considered uncomfortable and lengthy (especially for long or sinuous organs), it is still a preferred method in clinical practice as it ensures robustness and allows complete control. Topological thinning generates the exploration trajectory by eliminating layers of voxels (peeling) until the last one-voxel-thin core[1]. This last layer is designated to be the object skeleton, and represents one of the possible solutions of centerline extraction problem. One key and resource-demanding element of the iterative process is continuously finding the set of voxels (simple points) whose deletion does not modify the object topology.

The underlying idea of distance-map based methods is to make direct use of what can be called the "lateral information", that is, the distance of each composing voxel to its closest boundary[2]. The path is ideally placed along the map singularities (ridges). Difficult problems arise in case of complex geometries, when significant local maxima appear. Various variants have been proposed to cope with these cases[3,4], for example refining initially multi-branched graphs whose nodes are placed in the local maxima [5].

While in clinical practice the manual generation is still preferred, the various automatic algorithms proposed in the academic literature offer various degrees of solution stability. Actually, the two main classes of automatic generation algorithms (topological erosion, and distance field based) allow different approaches in pure and hybrid forms. A common characteristic of the majority of these methods is the usage of the lateral information, and the lack or insufficient usage of the information from the advancing direction – that we can call forward-looking information.

The algorithm proposed in this paper introduces a hybrid solution starting from the distance map method, in combination with the forward-looking concept. In essence, the approach is drawn upon natural ways of analysis and synthesis proper to human brain, as used for dynamic guidance during the advancement through tubular structures.

2 Algorithm description

The forward-looking information is obtained by a radial scanning of the distance map of the object, combined with variable-depth evaluations of the objective function. We obtain the optimal advancement direction by capturing in the objective function the two types of information discussed above. The algorithm is in the testing and tuning phase, aiming to achieve maximal stability based on the optimal definition of the hybrid objective function. Since the radial scanning procedure involves a negligible computation effort, the overall computing burden is comparable with that of applying a distance map filter.

a. *Data preparation and distance map generation*

The centerline algorithm receives as input the (3D) image of the segmented organ. A down-sampling step is applied first, depending on the nature and average cross-section of the investigated organ. This reduces the computation effort, enhances the solution stability, while keeping the quality of the result.

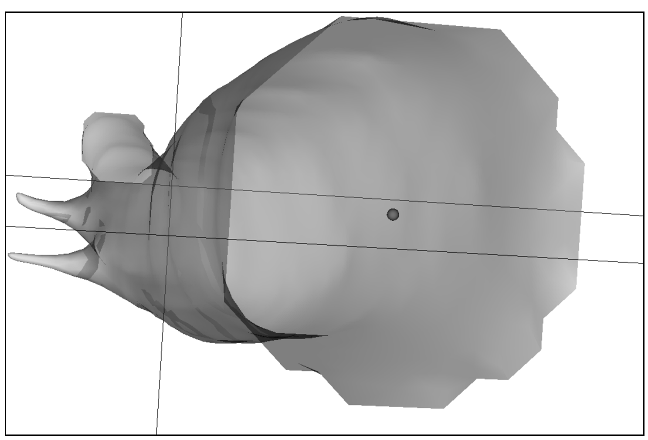

Figure 1: Orientation setting for start point selection. The start point is manually inserted

Next, a distance map algorithm is applied. There is no restriction on the chosen metric, and we investigate using lower-order metrics to speed-up the computation. The result of applying the distance map filter is a new image where the intensity of each inner voxel represents the distance to the closest boundary voxel. That is, the main ridge will appear in the center of the investigated structure.

b. *Initialisation of the scanning procedure*

This step involves the only operator intervention involved by the method. The operator designates a start point by mouse-picking it from the 3D domain. In beforehand, the image is rotated such that the plan of the starting section lies approximately parallel to the display. In this way, the program is able to record also the start direction as the direction perpendicular to the starting plane. This reorientation is achieved by simple mouse interaction, and the optimal visual assessment is simplified by offering the operator the triangulated model (Fig. 1), instead of the segmented model used in the previous steps. The start point and this initial direction determine the initial segment of the center line.

c. *Scanned forward-looking structure*

Each current point of the centerline will have associated a current direction vector. Given each current point and direction, for the calculation of the next pair a special forward-looking structure is created.

In this purpose we employ a ray-hemisphere (Fig. 2) centered in the current point. Uniformly distributed scanning rays are virtually generated with $\Delta\theta = \Delta\varphi$ longitude-latitude steps. The radial scanning angle is chosen according to the complexity of the anatomic structure. A sharp angular step ensures a detailed scanning with the price of quadratic increase of computation effort.

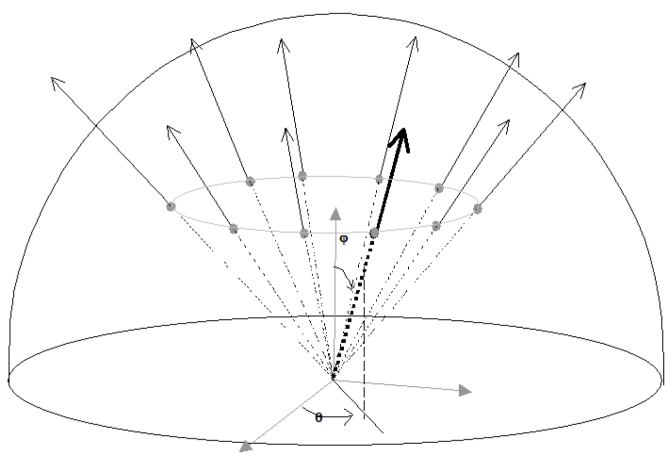

Figure 2: Forward-looking structure with uniformly distributed scanning rays

d. *Defining and computing the objective function*

To determine the optimal direction of advancement, an objective function must be defined, that combines both the lateral, and the forward-looking information. One can observe that:

- on the one side, the optimal advancing ray must "gather" (or "see") a distance-function value as large as possible along its path, ensuring in this way a maximal distance to the boundaries;
- on the other side, the optimal ray must have an inner route as long as possible, ensuring the advancement in the desired direction and not to the side walls;
- one must consider also the possibility to encounter organ curvatures, in which case a long inner ray *or* a large value of accumulated distance-function do not always represent the best trajectory;

- other special cases are represented by the occurrence of local maxima (caused, e.g., by haustral variations in structure diameter); or encountering sudden decrease of cross-section area, causing a decrease of the distance-function but still corresponding to the optimal advancement direction.

Taking into account all these observations, it can be seen that the optimal choice of the next point must take into account both the distance to the lateral walls, and the length of the forward projected rays.

Based on Fig. 3, we define the objective function in point p^k_j of the segment s_k as:

$$F(p_j^k) = D_{med}(p_j^k) \cdot L_k \quad (1)$$

where $D_{med}(p^k_j)$ is the average cumulated value of the distance-function, evaluated in the points $p^k_1,..,p^k_j$ and L_k represents the inner length of the s_k ray; for reasonably short sampling steps δ (relative to the estimated minimal cross-section diameter), L_k can be approximated with:

$$L_k \cong \delta \cdot M_k \quad (2)$$

The final expression of the objective function in the p^k_j scanning point is:

$$F(p_j^k) = \frac{M_k}{j} \sum_{i=1}^{j} D(p_i^k) \quad (3)$$

where $D(p^k_i)$ represents the value of distance-function in p^k_i.

e. *Finding the next point and direction vector*

The objective is to find the direction (ray) on which the advancement to the next point is to be performed. The imposed condition is to maximize the objective function (3). The maximum is searched over the "j" sampling points from each ray "k", that is over the set of p^k_j points, where: $k=1...N$, $j=1...M_k$. Thus, the advancement direction S_{opt} is determined as:

$$s_{opt} = \{ s_k \mid F(p_j^k) = \max; k = 1...N, j = 1...M_k \} \quad (4)$$

Any S_{opt} pointing backward related to the last centerline segment is discarded and the next optimum is considered. To maximize the stability, the next point along S_{opt} will be placed at a fixed step from the previous point. Also, the advancement direction is determined as an average (composition) of the previous direction with the direction of the optimal ray S_{opt} determined by (4).

The previous steps are repeated until an end condition is fulfilled; for example, when the total length of the centerline exceeds a specified limit, or when the segmented region is out-distanced. The estimated centerline is then smoothed by spline interpolation to ensure a smooth displacement of the virtual camera.

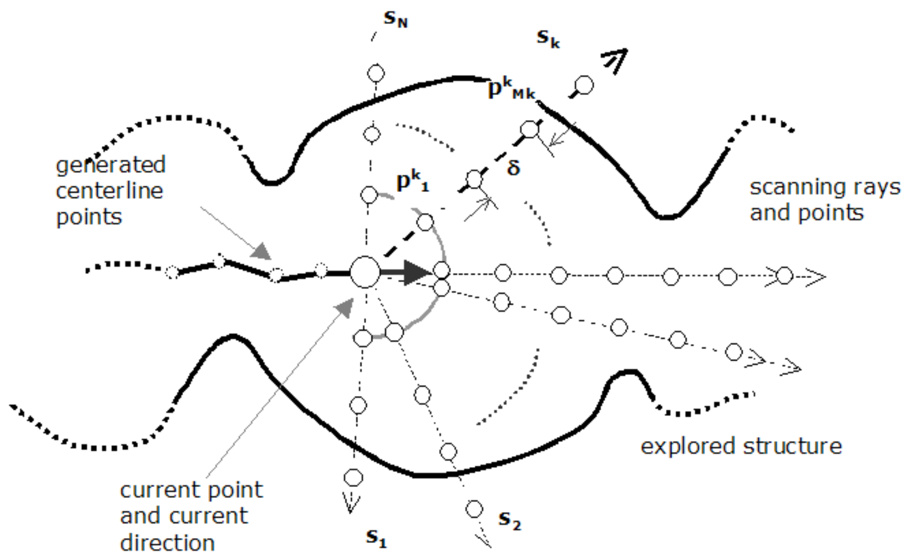

Figure 3: Sampling points $p^k{}_1 \dots p^k{}_{Mk}$, for the evaluation of the distance-function along each ray S_k $(k=1 \dots N)$

3 Results

We present here two results for simple and bifurcated tubular structures. In Fig. 4, for an aorta section, obtained after segmentation from MRI raw data: 37 points in centerline set, obtained in 1.5 sec. on a computer with dual-core CPU, 1.8 GHz clock speed.

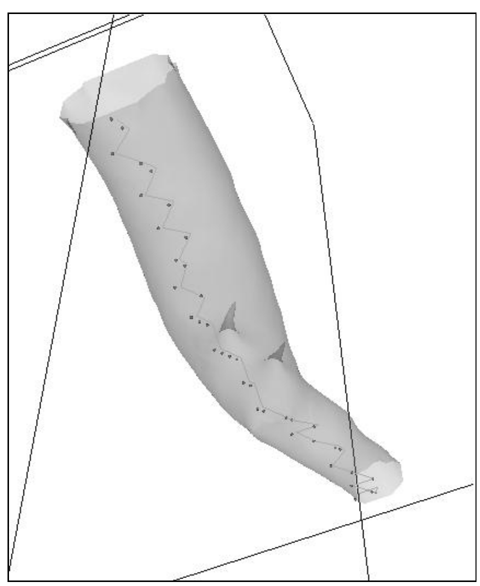

Figure 4: Centerline detection for simple, non-bifurcating tubular structure

In Fig. 5, from CT with contrast substance - raw data, 71 slices 512 $\times$ 512, for the aorta bifurcated in iliac arteries, we extracted the 64 points centerline in 5.5 sec. on a computer with dual-core CPU, 1.8 GHz clock speed.

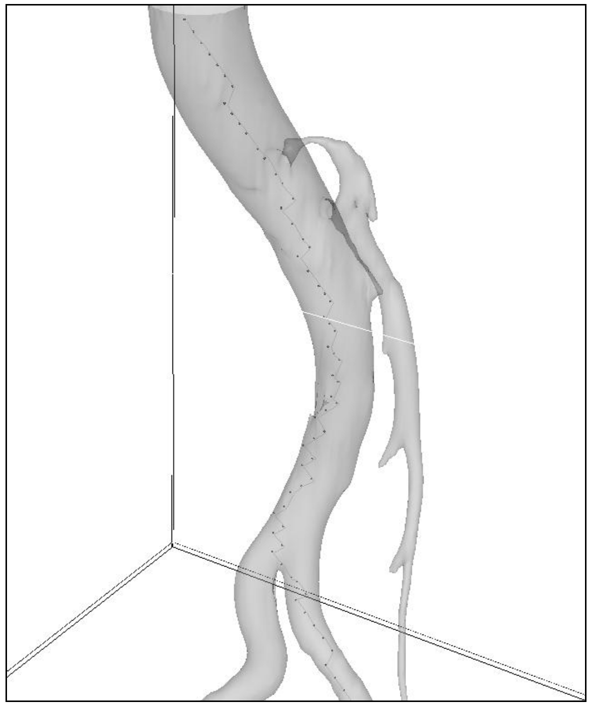

Figure 5: Centerline detection for bifurcating tubular structure (aorta bifurcating in iliac arteries)

4 Conclusion

A hybrid method for robust and efficient centerline generation was proposed. Similar to the brain analysis and synthesis of spatial information for orientation scenarios in closed spaces, the algorithm combines lateral position information with forward-looking information to decide the next step inside the inspected structure. The method was validated and tuned on various cavity organs.

References

[1] D.S. Paik, C.F. Beaulieu, R.B. Jeffrey, Jr., G.D. Rubin, S. Napel, Automated Flight Path Planning for Virtual Endoscopy, *Medical Physics* 25(5), 1998, pp. 629-637.

[2] M.W. Jones, J.A. Bærentzen, and M. Sramek, 3D Distance Fields: A Survey of Techniques and Applications, *IEEE Trans. Vis. Comput. Graph.,* 12(4), 2006, pp. 581-599.

[3] T. Deschamps, and L.D. Cohen, Fast extraction of minimal paths in 3D images and applications to virtual endoscopy, *Medical Image Analysis*, 5(4) , 2001, pp. 281-299.

[4] P. Chaudhuri, R. Khandekar, D. Sethi, P. Kalra, An Efficient Central Path Algorithm for Virtual Navigation, *Proceedings of Computer Graphics International* (CGI'04), 2004, pp. 188 – 195.

[5] H. Frimmel, J. Näppi, and H. Yoshida, Fast and robust computation of colon centerline in CT colonography, *Medical Physics*, 31, 2004, pp. 3046-3056.

Acknowledgments - This work was supported by the Romanian Government grant 55 CEEX II 03/24.07.2006 “Advanced Medical Imaging System for Diagnose, Guidance and Pre- and Intra-Operative Intervention: Model, Simulation and Analysis in Virtual Endoscopy”.